

Comparison of 2D and 1D Approaches to Forward Problem in¹ Mine Detection

Thomas P. Weldon^a, Yuriy A. Gryazin^b, and Michael V. Klibanov^b

^aDept. of Electrical and Computer Engineering,
University of North Carolina at Charlotte,

^bDept. of Mathematics,
University of North Carolina at Charlotte,
9201 Univ. City Blvd.,
Charlotte, NC 28223, USA

ABSTRACT

Recently, we have successfully applied the Elliptic Systems Method to inverse problems in laser medical imaging applications. As part of applying this method to mine detection, accurate and fast algorithms are required for solving the forward problem to generate data for the inverse problem. Results for the two-dimensional forward problem using GMRES (Generalized Minimum Residual) method are compared with one-dimensional transmission line models. Simulation results for mines and clutter are provided for both methods. The comparison with one-dimensional results suggests that GMRES is an effective approach to modeling the forward problem in mine detection. In addition, the contrast between results for mines and clutter provide useful signal features for initial screening between mines and clutter.

Keywords: Land mine detection, GMRES, forward problem, transmission line models

1. INTRODUCTION

The detection of buried land mines remains a difficult and challenging inverse problem. The variability in soil conditions, mine composition, mine size, mine depth, and false targets such as stones further exacerbate the problem. To address this complex problem, we have proposed a novel overall approach to the inverse problem in land mine detection using the elliptic system method (ESM) recently developed by Klibanov et al.¹⁻³ for inverse problems in optical tomography. The ESM method provides fast and accurate solution of the inverse problem and is presently under development for land mine detection.¹ The present paper focuses on a novel forward method that is used to generate data in support of the development and testing of the ESM inverse method, and comparisons between the new method and a transmission line method. In addition, the transmission line method may lead to a simple computationally efficient pre-screening method for identifying suspicious targets, whereas ESM would provide more detailed analysis after a suspicious object is found.

The development of new methods for solving inverse problems frequently requires the solution of the forward problem to generate test data for evaluating the inverse methods. In earlier work, Gryazin et al.^{2,3} presented a novel forward method that provides fast and accurate solution of the forward problem for land mine detection. This approach is based on preconditioned GMRES method.⁴ In the present paper, we compare two-dimensional results for land mines using our new forward method to one-dimensional results using the transmission line methods presented by Trang.^{5,6} Experimental results generated by these two different methods are quite similar, even though the two-dimensional approach of the new method is significantly more complex than the one-dimensional transmission line method.

In the following sections, the physical scenario for a buried land mine is first described. The transmission-line method for modeling the land mine is given next. Then, the GMRES-based algorithm is summarized. Finally, results are presented for the two methods.

Further author information: (Send correspondence to T. Weldon), E-mail: tpweldon@unc.edu, Copyright 2000 Society of Photo-Optical Instrumentation Engineers. This paper was published in SPIE Proceedings, Aerosense 2000, April, 2000 and is made available as an electronic preprint with permission of SPIE. One print or electronic copy may be made for personal use only. Systematic or multiple reproduction, distribution to multiple locations via electronic or other means, duplication of any material in this paper for a fee or for commercial purposes, or modification of the content of the paper are prohibited.

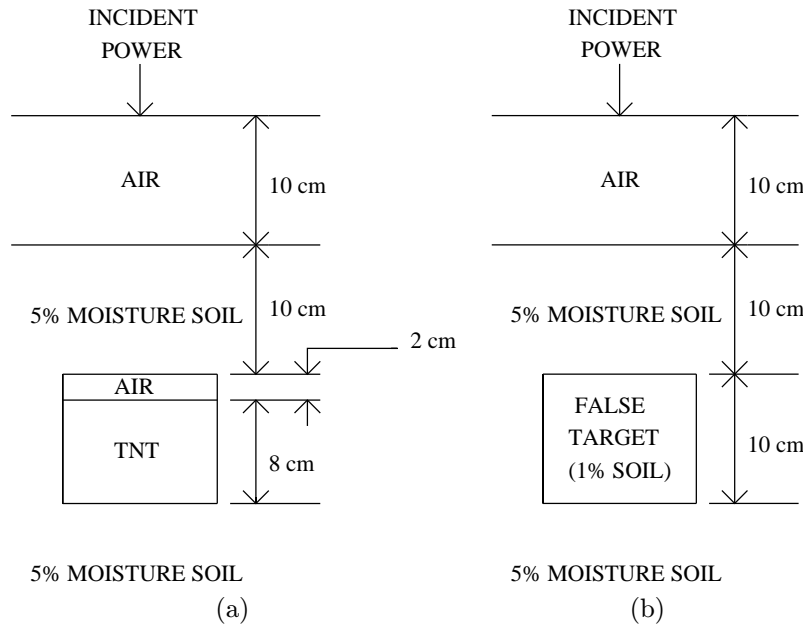


Figure 1. Physical scenario used for simulations. a) Land mine at 10 cm depth consisting of air gap and TNT. b) False target consisting of soil with 1% moisture buried at 10 cm depth.

2. PHYSICAL DESCRIPTION

The two-dimensional GMRES approach and the one-dimensional transmission line method were tested using two different physical scenarios. The first scenario is representative of a plastic land mine buried in soil of moderate moisture content. The second scenario replaces the land mine with a false target, or clutter. The two scenarios are described below. Simulation results using the two methods are presented later.

The physical scenario is illustrated in Fig. 1(a) for the case of a land mine. An electromagnetic plane wave is incident in air at a point 10 cm above the surface of the soil with the land mine 10 cm beneath the surface of the soil. A small air gap of 2 cm is assumed to exist within the top portion of the mine. The bottom 8 cm portion of the mine then consists of TNT explosive material. The effects of casing materials are omitted since a relatively thin plastic land mine casing is assumed. In any event, the omission of the casing does not affect the primary goal of comparing results for the two simulation methods. Finally, the mine is completely surrounded by soil on all sides.

In the second physical scenario of Fig. 1(b), the land mine is replaced by a false target, or clutter, with the same overall dimensions as the land mine. A relatively simple false target was constructed by using the parameters for soil with lower moisture content than the surrounding soil. This model embodies the main features of a difficult false target with similar dimensions to the land mine and differing only in composition. Even though the dry soil may not necessarily be representative of a stone, for instance, it is useful for illustrating the qualitative effects of a false target. In addition, the scenario of Fig. 1(b) provides a second physical system for the purposes of comparing the two simulation methods.

3. TRANSMISSION LINE METHOD

The first method for simulating the two scenarios of the previous section follows the approach presented by Trang.^{5,6} In this approach, each of the regions of electromagnetic propagation is modeled as a section of transmission line. This results in a one-dimensional model of the problem. Although the geometry effects of a more complicated two-dimensional model are not included, the transmission line method provides a simple baseline model that can be easily

simulated using SPICE electrical simulation software. In the development below, the electromagnetic equations for free space propagation are first compared to the equations for propagation along a transmission line. Equivalent parameters for the transmission line model are then given in terms of the parameters of the materials in each region.

Plane wave propagation in the y direction for lossy dielectrics is given by⁷

$$E = E_0 e^{-\gamma y} = E_0 e^{-\alpha y} e^{-j \beta y} \quad (1)$$

where E_0 is the incident complex phasor electric field at $y = 0$, and α and β are attenuation and phase constants for the material in which the electromagnetic wave is propagating. The propagation constant γ in a lossy dielectric with permittivity $\epsilon = \epsilon_r \epsilon_0$, conductivity σ , and permeability $\mu = \mu_r \mu_0$, is given by is then

$$\gamma = \sqrt{j \omega \mu (\sigma + j \omega \epsilon)} \quad (2)$$

where $j = \sqrt{-1}$, μ is magnetic permeability in Henry/m, σ is conductivity in Siemens/meter, ω is the angular frequency of the radiation in radians per second, and ϵ is the dielectric constant in Farads/m. The free space constants are $\mu_0 = 4\pi \times 10^{-7}$ H/m and $\epsilon_0 = 8.85 \times 10^{-12}$ F/m, μ_r is relative permeability, and ϵ_r is the relative permittivity of the material.

The dielectric losses are commonly expressed as a loss tangent that is related to the foregoing parameters using

$$\tan \delta = \frac{1}{\sqrt{\omega \epsilon}} \quad (3)$$

The foregoing equations for propagation in free space are directly analogous to the equations for propagation in transmission lines, with the electric field E and magnetic field H replaced by the voltage V and current I along a transmission line. Following the above development for the electric field E , the voltage V along a transmission line is⁷

$$V = V_0 e^{-\gamma y} \quad (4)$$

where V is the voltage at position y from the source and V_0 is the incident voltage at $y = 0$. The propagation constant γ for the transmission line is

$$\gamma = \sqrt{(R + j \omega L)(G + j \omega C)} \quad (5)$$

where R is resistance per unit length in Ohm/m, L is inductance per unit length in Henry/m, G is conductance per unit length in Siemens/m, and C is capacitance per unit length in Farads/m for the transmission line.

Comparing the free space and transmission line equations, they are identical if $V = E$, $I = H$, $R = 0$, $L = \mu$, $G = \sigma$, and $C = \epsilon$. Thus, the plane wave propagation in Eq. 1 can be modeled using transmission line equations Eq. 4 and electronic simulation software such as SPICE.

The physical scenario of Fig. 1(b) is then modeled using the transmission line system of Fig. 2. Each material is modeled as a section of transmission line with a physical length equal to the y , or vertical, dimension of the material in Fig. 1(b). A corresponding transmission line model for Fig. 1(a) would replace the 1% moisture soil section with a 2 cm air line section followed by an 8 cm TNT transmission line section.

The parameters for the materials used in our experiments are given in Table 1.⁸

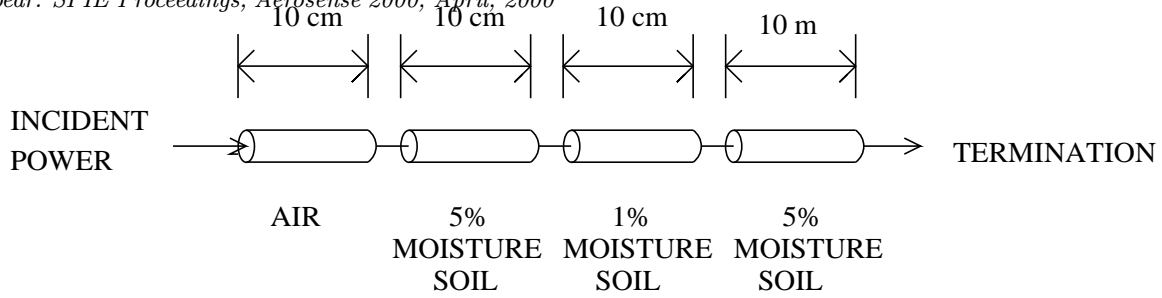


Figure 2. Transmission line sections corresponding to false target, or clutter, at 10 cm depth.

Table 1. Parameters used in simulations.

Parameter	Air	5% Moisture Soil	1% Moisture Soil	TNT	Units
$\epsilon = C$	8.85	35.4	25.7	25.3	pF/m
$\mu = L$	1.26	1.26	1.26	1.26	μ H/m
$\sigma = G$	0	0.049	0.004	0.00029	S/m

4. GMRES-BASED METHOD

In recent work, Gryazin et al.² have developed a new algorithm based on GMRES method that provides fast and accurate simulation for solving the forward problem. In this new approach, the GMRES method is improved by using a carefully chosen preconditioner. This new method helps overcome computational difficulties that arise due to the large number of grid points necessary in solving the Helmholtz equations for the land mine problem at high frequencies. A brief summary of the method is given below, and further details are found in the related paper.²

The boundary value problem is governed by the Helmholtz equation

$$\nabla^2 E + \gamma^2(x, y) E = 0 \quad (x, y) \in \Omega \quad (6)$$

where $\gamma^2(x, y)$ is again the propagation constant as a function of (x, y) coordinates, Ω is the region where the solution is found, and E is the electric field previously described. Instead of Sommerfeld boundary conditions at infinity, an approximation to it is imposed on the boundary of the auxiliary domain Ω :

$$\frac{\partial E}{\partial n} - j\gamma E = 0 \quad (7)$$

where $\frac{\partial E}{\partial n}$ is the derivative electric field normal to the boundary of Ω in an outward direction.

The problem is then discretized using a second order finite difference scheme to compute the solution on a regular mesh in Ω . The resulting matrix describing the system of equations has a block tridiagonal structure but is neither positive definite nor Hermitian. Thus, most iterative methods of solution exhibit convergence problems or are converge too slowly for the large number of mesh points required at high frequencies.

These computational difficulties are addressed by using the GMRES method with a preconditioner that uses Sommerfeld-like boundary conditions (7) at the upper and lower y-axis boundaries and Dirichlet or Neumann boundary conditions at the left and right x-axis boundaries. This results in a fast and accurate algorithm for computing the solution of the Helmholtz equation. The effect of using Sommerfeld-like boundary conditions on the boundary of

the auxiliary domain Ω rather than Sommerfeld conditions at infinity is minimized by increasing the size of Ω until the solution well within Ω does not change significantly. This approach works particularly well when the attenuation characteristics of the soil are high, leading to low values of the electric field at the boundaries. The solution of the equation in three dimensions is prohibitive, and for the purposes of this paper the equation is solved in two dimensions for the scenarios of Fig. 1. In the simulations, a mesh of 400×400 points within a $1 \text{ m} \times 1 \text{ m}$ region Ω is used with a width of 20 cm for both the mine and false targets in Fig. 1.

Finally, the approach to the simulation is to solve for the perturbation of the solution $E(x, y)$ when a land mine is present relative to the solution with no mine. Let $E_0(x, y)$ be the solution when no mine is present and $E_m(x, y)$ be the solution when the mine is present. The solution $E_0(x, y)$ is well known since it corresponds to a plane wave solution between two different media, soil and air. The perturbation $E_p(x, y)$ defined as

$$E_p(x, y) = E_m(x, y) - E_0(x, y) . \quad (8)$$

Substituting into the Helmholtz equation results in

$$\nabla^2 E_m + \gamma^2(x, y) E_m = -f(x, y, E_0) \quad (x, y) \in \Omega \quad (9)$$

where

$$f(x, y, E_0) = \begin{cases} f(x, y, E_0) = 0 \\ f(x, y, E_0) = (\gamma^2 - \gamma_0^2)E_0 \end{cases} \quad (x, y) \in \text{land mine region} \quad (10)$$

The land mine is presumed to lie well inside the spatial region Ω where the solution is computed. This system is then solved using GMRES and the aforementioned preconditioner and boundary conditions. Further details of this new method can be found in Gryazin et al..² The result is the perturbation in the electric field $E_p(x, y)$ caused by the presence of a min or other target.

5. EXPERIMENTAL RESULTS

Simulation results using the one-dimensional transmission line method are given in Fig. 3. Since the GMRES method gives the perturbation of the E field relative to the E field when a mine or when a false target is not present, the transmission line results in Fig. 3 are adjusted to give the perturbation also. This is accomplished by subtracting the transmission line solution when no mine nor false target is present from the solution obtained when the mine or false target is present. Since the GMRES-based method generates results in the frequency domain, the transmission line results are plotted as a function of frequency.

The plot in Fig. 3(a) shows the perturbation in the transmission line voltage V at the incident power location corresponding to a point 10 cm above the soil in Fig. 1(a). The frequency is varied from 750 MHz to 3 GHz with the magnitude of the perturbation voltage normalized to a 1 volt incident power source. Fig. 3(b) gives the perturbation resulting for the false target of Fig. 1(b).

Similarly, the GMRES-based method was used to generate the results of Fig. 4. The plots in Fig. 3 show the perturbation in the E field at the incident power location corresponding to a point 10 cm above the soil in Fig. 1(a) and along the midline of the land mine. The perturbation normalized to a $E = 1$. The case of the land mine is given in Fig. 4(a) and the case of a false target is given in Fig. 4(b). In Fig. 4 the width of the land mine and false target were 20 cm.

Comparing Fig. 3 and Fig. 4, the two methods generate results with similar magnitude and frequency response. Moderate differences between the two methods are not unexpected, since the GMRES-based method provides a two-dimensional model of the scattering of the electromagnetic signal from the targets. The one-dimensional transmission

line model, being greatly simplified, does not account for effects associated with the two-dimensional geometry of the land mine. Nevertheless, there is significant agreement between the two methods.

The large differences in results in Fig. 3(a) and Fig. 3(b) suggest that the transmission line method may lead to a simple and computationally inexpensive prescreening for the presence of mines. This could lead to an effective mine detection system where the ESM method would be employed for detailed analysis after a suspicious object is identified using more simple transmission line methods.

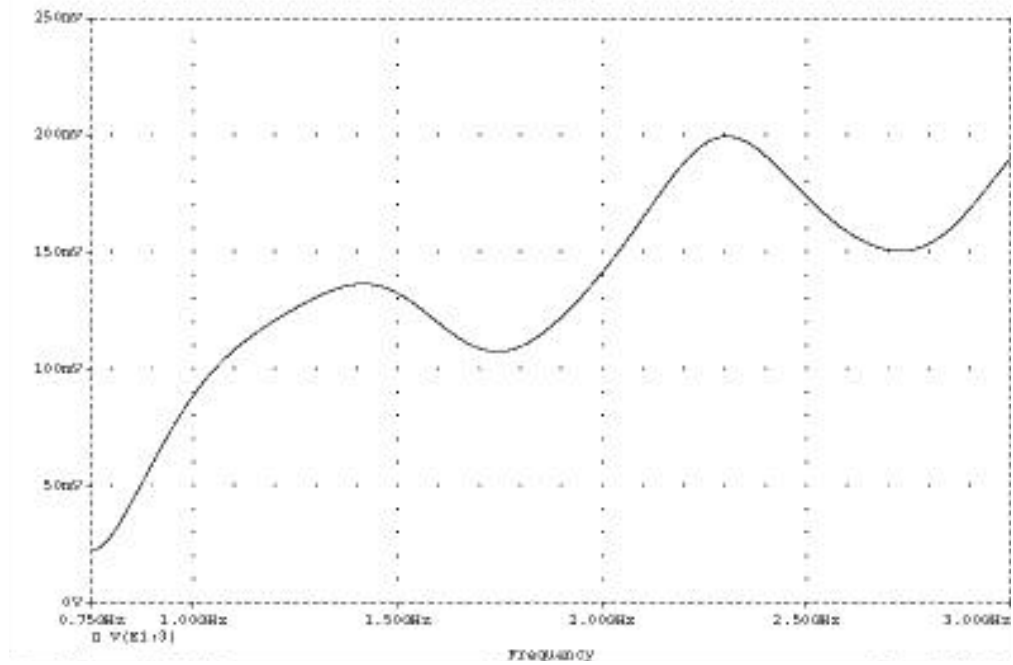
Finally, the transmission line model allows a simple time domain solution using electronic simulation software. Fig. 5 gives transmission line time-domain results for the land mine and false target. In Fig. 5(a), it is difficult to differentiate the components of the target reflections from the land mine because of poor temporal separation in reflections from the air gap and TNT. In Fig. 5(b), the incident pulse is a single cycle at 2GHz at 2 Volts peak-peak. The first reflection at 0.67 ns is from the air-soil interface. The second and third reflections at 2.0 and 3.2 ns are from the top and bottom of the false target.

ACKNOWLEDGMENTS

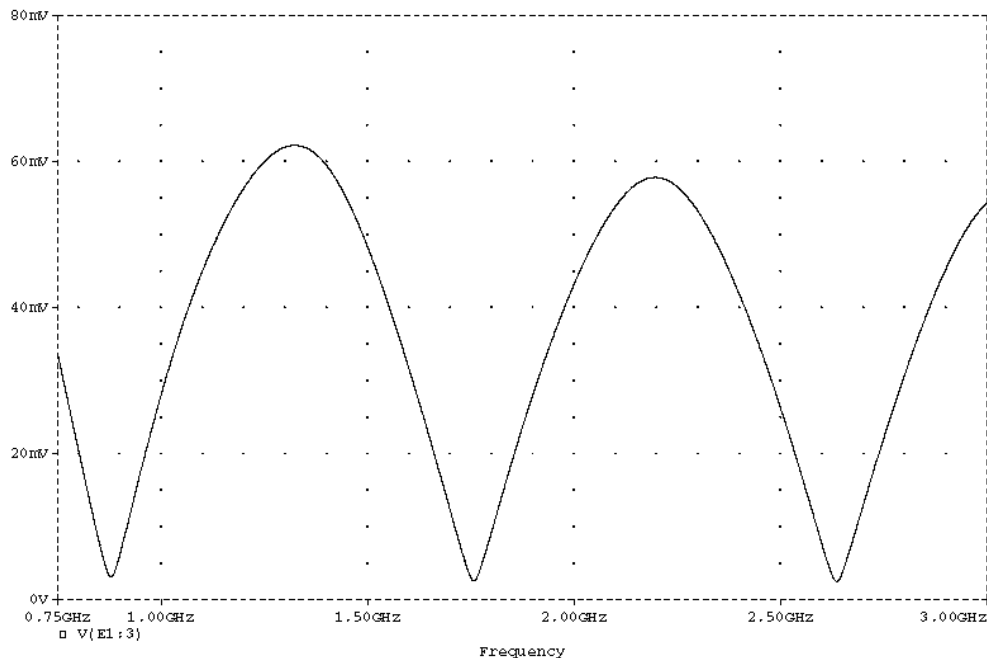
This work is partially supported by the U.S. Army Research Office grant DAAG 55-98-1-0401.

REFERENCES

1. M. V. Klibanov, T. R. Lucas, and R. M. Frank, "A fast and accurate imaging algorithm in optical diffusion tomography," *Inverse Problems* **13**, pp. 1341–1361, 1997.
2. Y. A. Gryazin, M. V. Klibanov, and T. R. Lucas, "GMRES computation of high frequency electrical field propagation in land mine detection," *Journal of Computational Physics* **158**, pp. 1–18, Jan. 2000.
3. Y. A. Gryazin, M. V. Klibanov, and T. R. Lucas, "Imaging the diffusion coefficient in a parabolic inverse problem in optical tomography," *Inverse Problems* **15**, pp. 373–397, 1999.
4. Y. Saad and M. H. Schultz, "GMRES: A generalized minimum residual algorithm for solving nonsymmetric linear systems," *SIAM J. Sci. Statist. Comput.* **7**, p. 856, 1986.
5. A. H. Trang, "Simulation of mine detection over dry soil, snow, ice, and water," in *SPIE Proceedings*, vol. 2765, pp. 430–440, Apr. 1996.
6. A. H. Trang, "Simulation of close-in and stand-off mine detection," in *IGARSS'97, 1997 International Geoscience and Remote Sensing Symposium*, pp. 1132–1134, 1997.
7. W. H. Hayt, *Engineering Electromagnetics*, McGraw Hill, 3rd ed., 1974.
8. "Dielectric constants and loss tangents of explosives." data of U.S. Army Belvoir RD&E Center.
9. A. Y. Rathore, *Wave Propagation Model and Simulations For Landmine Detection Using Ground Penetrating Radar*. MS thesis, Univ. of N. Carolina at Charlotte, 1999.



(a)



(b)

Figure 3. Transmission line frequency response. a) Land mine at 10 cm depth. b) False target at 10 cm depth.

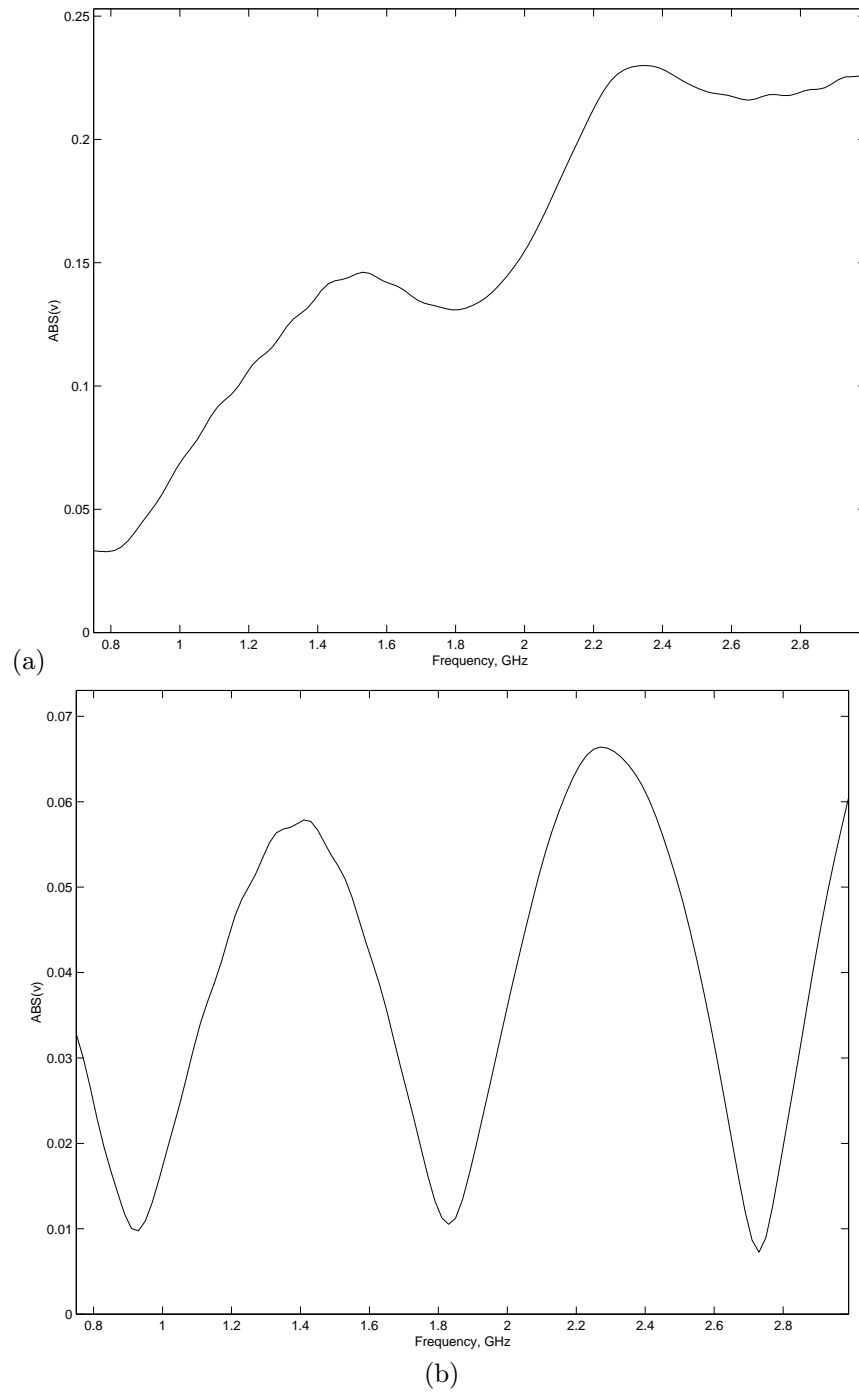
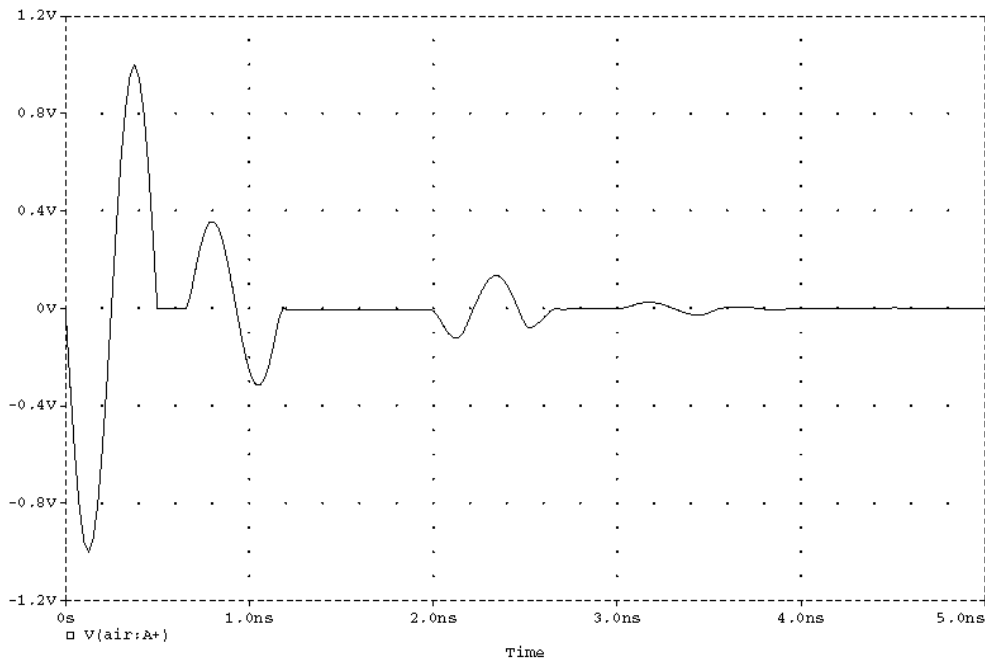
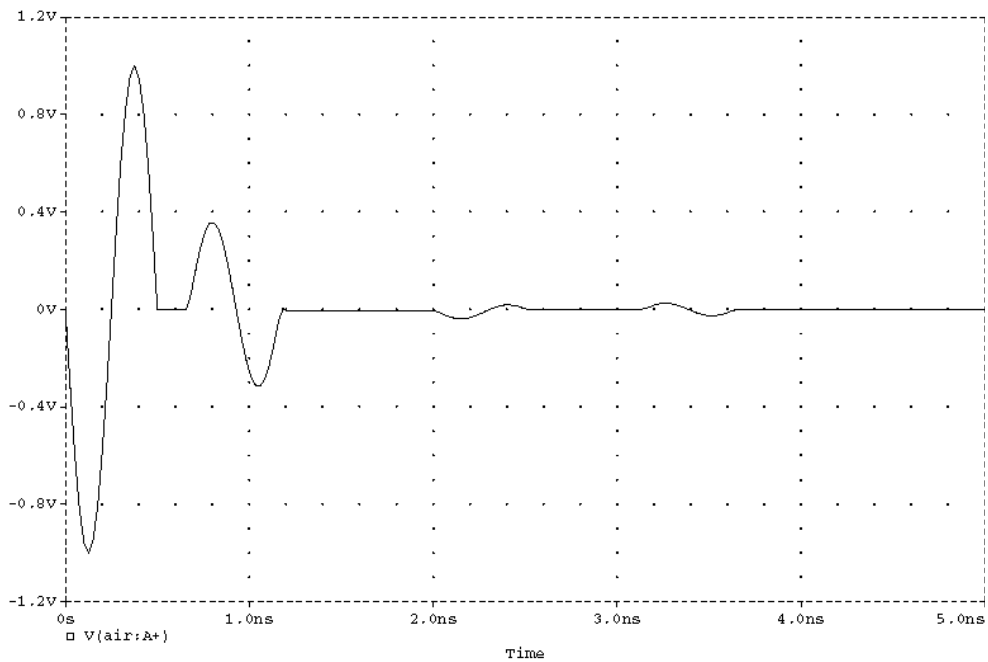


Figure 4. GMRES-based frequency response. a) Land mine at 10 cm depth. b) False target at 10 cm depth.



(a)



(b)

Figure 5. Transmission line time-domain results. a) Mine at 10 cm depth. b) False target at 10 cm depth. Incident pulse is a single cycle at 2GHz at 2 Volts peak-peak. First reflection at 0.67 ns is from air-soil interface. Second and third reflections at 2.0 and 3.2 ns are from the top and bottom of the false target.